# Short-Range Ordered Aluminum Foams

*Ningzhen Wang, Mike Andreas Noack, Paul Hans Kamm, John Banhart, and Francisco García-Moreno\**

Ordering the bubbles of closed-cell aluminum foams can contribute to decorative esthetics and create directional mechanical properties that disordered foams do not have. High-porosity (>80%) aluminum foams prepared by the traditional static gas injection method usually have large and polyhedral cells, which do not form an ordered stacking. Aluminum foams with relatively uniform and small cells (cell size ≈1.2 mm) have been recently obtained by gas injection through a nozzle rotating at high speed. Herein, the stacking of aluminum foams with different cell sizes and a monodisperse aqueous foam are characterized by X-ray tomography and compared with an ideal face-centered cubic (FCC) structure. The aluminum foam featuring the smallest cells has a concentrated distribution of cell coordination number with a peak of 12 and the first peaks of the radial distribution function are found to be consistent with those of the monodisperse aqueous foam and an ideal FCC structure. Furthermore, many aligned bubble chains with more than five bubbles are observed on cross-sectional images. Therefore, aluminum foam can become short-range ordered whenever the cell size is uniform enough and reduced to around 1.2 mm. Methods for further improving the order of aluminum foam are discussed.

## 1. Introduction

Closed-cell solid aluminum foam consists of nonconnected pores embedded in a continuous aluminum phase.[1] The unique random foam structure and the lightweight nature of aluminum make it possible to combine properties such as high specific strength, energy absorption, electromagnetic shielding, noise reduction, and fire prevention capability in one material.[2] Therefore, aluminum foam is used in fields such as building decoration, aerospace, and automotive.[3,4] Foams with more ordered

structures can help to improve the esthetics, directional mechanical performance, and statistical reproducibility of properties of disordered aluminum foam. Obtaining ordered foam structures has far-reaching significance in expanding the applications of aluminum foams. The cells of aluminum foams made by melt foaming or powder metallurgy are often formed by the decomposition of a blowing agent (e.g., $TiH_2$, $ZrH_2$), so the foam structure is strongly influenced by the gas nucleation behavior and the size and dispersion of the blowing agent particles.[5,6] In contrast, by applying the gas injection method, cells are obtained by creating gas bubbles, which then rise to the melt top and accumulate there, after which the foam solidifies. This procedure is more conducive to the accumulation of bubbles into an ordered structure as they tend to choose a position of minimum free energy.[7,8] The available methods can be divided into dynamic and static gas injection according to whether the gas injection needle is moving or not, respectively.[9] The static gas injection method is beneficial for the uniformity of bubbles, but the cells are usually large (≥5 mm).[10] Large cells are easy to compress in the direction of gravity and become polyhedral.[11] Traditional rotating or reciprocating gas injection methods can reduce the bubble size to some extent, but the large disturbance to the melt causes poor cell size uniformity.[12,13] In addition, porosities of aluminum foams prepared by the traditional gas injection method are usually larger than 80%.[11] Large, nonspherical, and not uniformly distributed cells do not stack into an ordered foam structure.

For foams in general, ideal ordered stacking requires that the units should be spherical and monosized, which usually means a dense crystal packing and efficient packing state.[14] Research on ordered and dense packings has progressed a lot in condensed matter physics and physical chemistry.[15] For monosized hard spheres, the geometrical structure of random stackings in a large container and optimal dense packings in a thin cylinder have both been studied.[14,16,17] In addition, it was estimated that randomly stacked hard-sphere colloidal suspensions will anneal to face-centered cubic (FCC) structures after months or years.[18] In comparison, foam structures formed in confined cylinders were found to resemble close packings of hard spheres.[19] However, ordered packings of bubbles are more difficult to obtain compared to hard spheres as they are subject to drainage, coalescence, and coarsening during accumulation.[20] Most

N. Wang, M. A. Noack, J. Banhart, F. García-Moreno
Institute of Materials Science and Technology
Technische Universität Berlin
Hardenbergstraße 36, Berlin 10623, Germany
E-mail: garcia-moreno@helmholtz-berlin.de

P. H. Kamm, J. Banhart, F. García-Moreno
Institute of Applied Materials
Helmholtz-Zentrum Berlin für Materialien und Energie
Hahn-Meitner-Platz 1, Berlin 14109, Germany

The ORCID identification number(s) for the author(s) of this article can be found under https://doi.org/10.1002/adem.202100795.

**ADVANCED
SCIENCE NEWS**

www.advancedsciencenews.com

**ADVANCED
ENGINEERING
MATERIALS**

www.aem-journal.com

studies about ordered stackings of monosized bubbles are based on aqueous foams.[21–23] Bubbles can anneal to polydisperse or bidisperse states from the monodisperse system via a self-organizing effect.[22,24] It was also demonstrated that the close-packed FCC structure formed by monosized spherical bubbles transforms into a body-centered cubic (BCC) Kelvin structure with tetrakaidecahedron-shaped bubbles as the liquid fraction decreases.[23] García-Moreno et al. disclosed that the meniscus shape caused by the surface tension of columnar aqueous foam will also lead to a deviation from an ideal structure.[25] Meagher et al. found an FCC structure on the surface of a large foam sample, whereas a random packing was seen in its interior.[26] Despite the difficulty of obtaining ordered packings of bubbles, it was reported that a monodisperse and disordered foam can evolve into FCC or HCP (hexagonal close packed) structure in several days when coarsening of bubbles is inhibited.[27] Therefore, increasing the stability of bubbles is important for forming an ordered foam. Drainage is slower and coarsening can be controlled using the proper surfactant and blowing gas when the bubbles are small enough.[20,28] Therefore, reducing bubble size appears to be a necessary and effective method to obtain stable bubbles.

For aluminum melts, individual films of smaller areas have been found to be more stable, which correspond to smaller bubbles in a foam.[29] In addition, smaller bubbles are assumed to be more spherical on the basis of the Young–Laplace equation.[8] Therefore, preparing aluminum foams with small, spherical, and uniform cells with the gas injection method is an essential challenge and opportunity for achieving ordered foam structure. Babcsán et al. obtained aluminum foams with submillimeter-sized pores by adding ultrafine stabilizing particles to an aluminum melt and introducing ultrasonic vibration during preparation.[30–32] García-Moreno et al. attained small bubbles by reducing the equivalent area of gas-injecting cannulae, optimizing the cannula shapes and applying oscillations to the cannulae.[8] They also observed that small and uniform bubbles aligned in chains, which implies an initial formation of ordered

foam structures.[8] Wang et al. reduced the bubble size by applying high-speed horizontal oscillations to the gas injection needle and improving the foamable melt, wherein uniform cells can be obtained under specific vibration conditions.[9,33] Based on this research on small-cell aluminum foam, it is worthwhile and interesting to further explore whether closed-cell aluminum foam can achieve an ordered foam structure.

In this work, aluminum foams with small cells prepared by a newly developed high-speed rotation method were studied. For comparison, stacking structures of an aluminum foam prepared by static gas injection and an aqueous foam with ultrafine bubbles were also analyzed. Nondestructive X-ray tomography was applied to obtain quantitative 3D data of the foam structure along with the volume, shape parameter, and position of bubbles. The degree of bubble stacking order was characterized by the coordination number and the radial distribution function. An aluminum foam with ≈1.2 mm cell size prepared by the high-speed rotation method was verified to have a short-range ordered structure. Methods to improve the degree of order of the foam are proposed.

## 2. Results

### 2.1. Characterization of Foam Structures

After preparing the four foams by gas injection, the part of the foam containing fine bubbles or cells was extracted by Avizo for studying cell stacking. Overall porosities of the four extracted foam samples range from 71% to 76%. 3D rendered tomographic images of the foams are shown in **Figure 1**, where different colors denote separated cells. **Figure 2** shows the fraction of the cell volume in a given equivalent cell diameter range relative to the entire volume. Despite the large amount of micropores in the samples, especially for Alumi-fast and Alumi-slow caused by the disturbance of the melt during preparation,[34,35] their volume fraction in the whole foam is still small enough in Figure 2. Therefore, cells with equivalent diameters below 0.5 mm for Alumi-fast, 0.5 mm for Alumi-slow, 1.25 mm for Alu-static,
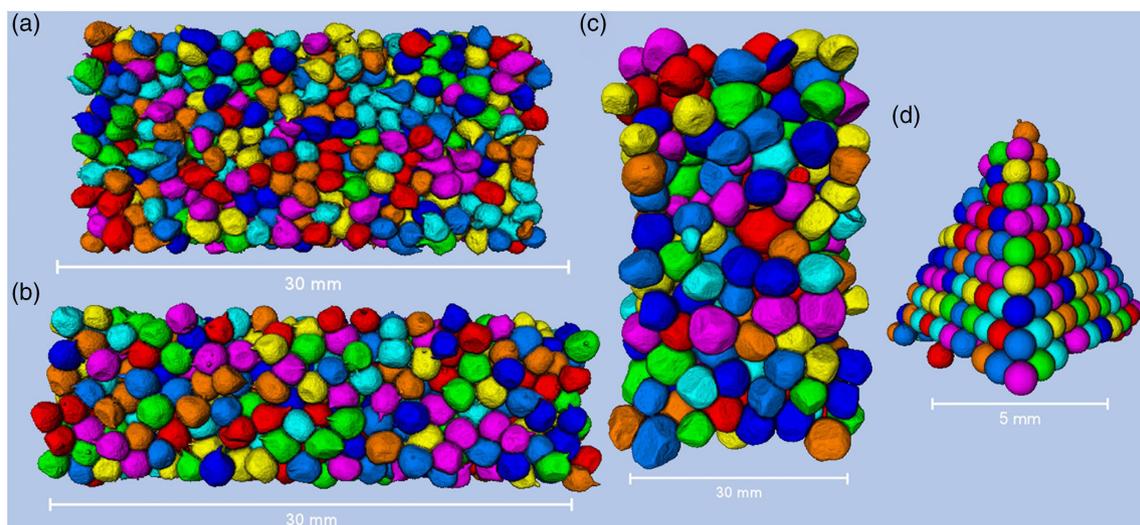


**Figure 1.** 3D rendered images of the extracted cells in a) Alumi-fast, b) Alumi-slow, c) Alumi-static, and d) the Aqueous foam as obtained by X-ray tomography.
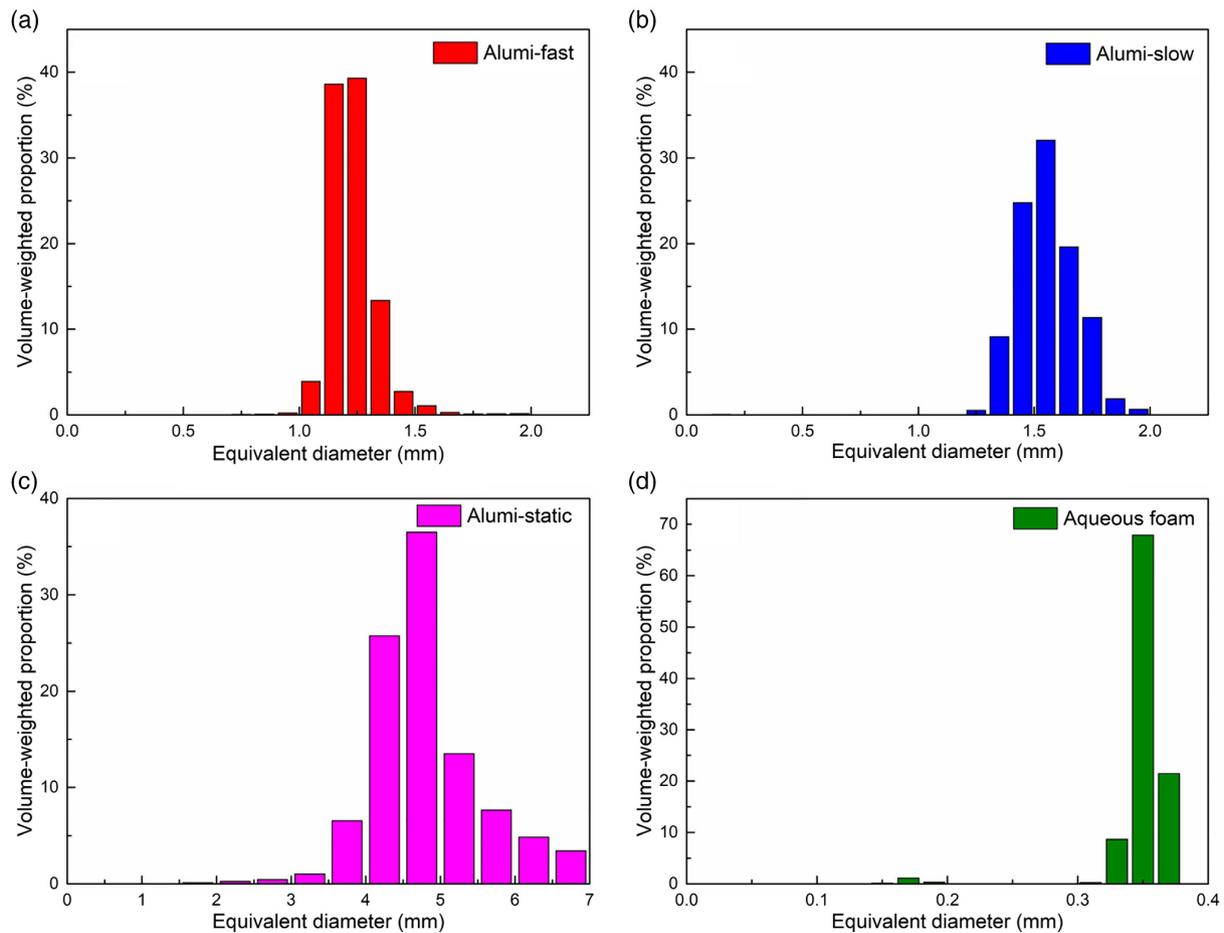
**ADVANCED
SCIENCE NEWS**
www.advancedsciencenews.com

**ADVANCED
ENGINEERING
MATERIALS**
www.aem-journal.com

**Figure 2.** Volume-weighted normalized distribution of equivalent cell diameters of a) Alumi-fast, b) Alumi-slow, c) Alumi-static, and d) the Aqueous foam.

and 0.25 mm for the Aqueous foam were classified as micropores—their volume fractions are 0.01%, 0.08%, 0.02%, and 1.7%, respectively—which should not affect the stacking state of foams, and were removed and neglected in the following cell stacking analysis. The cell size parameters of the four foams can be found in **Table 1**. There is little difference between the average and median equivalent cell diameters, and the average cell diameter was used to represent the cell size of the samples in the following.

As shown in Figure 1 and 2, Alumi-fast has the smallest cell size and the narrowest cell size distribution among the three aluminum foam samples. Alumi-static has the largest average cell diameter and many cells are polyhedral. Because of the higher gas flow rate and lower rotation speed during preparation compared to Alumi-fast, the cell size of Alumi-slow is larger and the cell size uniformity is lower. Therefore, the newly developed high-speed rotation gas injection method successfully reduces the cell size of aluminum foam, in this case to $1.21 \pm 0.09$ mm, and ensures good foam uniformity. The bubble size of the Aqueous foam is smaller ($0.35 \pm 0.01$ mm) yet, determined by the surface tension and viscosity of the aqueous solution. The uniformity of bubble size in the Aqueous foam is also very pronounced due to the static gas-injecting condition and existence of efficient surfactants.

**Table 1.** Statistical cell structural parameters of the four foam samples.

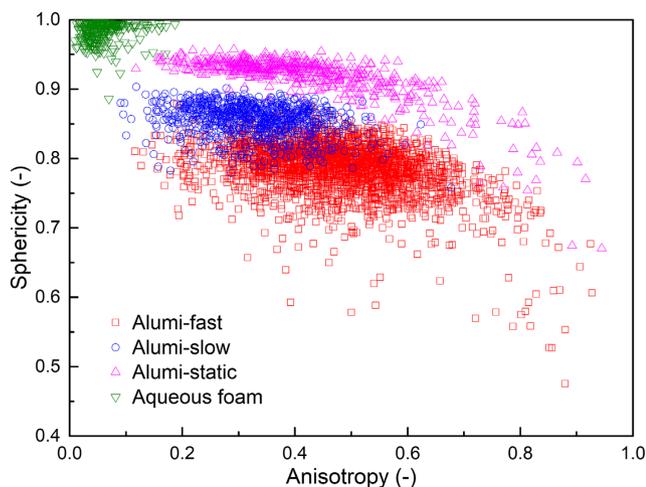| Samples | Porosity [%] | Equivalent diameter [mm] | | | Cell sphericity | | Cell anisotropy | |
|---|---|---|---|---|---|---|---|---|
| | | Average value | Standard deviation | Median value | Average value | Standard deviation | Average value | Standard deviation |
| Alumi-fast | 71 | 1.21 | 0.09 | 1.20 | 0.79 | 0.04 | 0.48 | 0.12 |
| Alumi-slow | 74 | 1.53 | 0.12 | 1.52 | 0.86 | 0.02 | 0.33 | 0.09 |
| Alumi-static | 76 | 4.41 | 0.83 | 4.49 | 0.92 | 0.03 | 0.42 | 0.14 |
| Aqueous foam | 71 | 0.35 | 0.01 | 0.35 | 0.98 | 0.01 | 0.06 | 0.03 |

**Figure 3.** Distribution of cell sphericity versus cell anisotropy of the four foam samples. Perfect spheres are located in the upper left corner.



**Figure 4.** Distribution frequency of cell coordination numbers in the four foam samples.

**Figure 3** shows the distribution of cell sphericity and anisotropy of the four foam samples, and the results of statistical analyses are displayed in Table 1. Figure 3 and Table 1 imply that the four foams can be arranged according to the similarity of their cells with an ideal sphere in the order: Aqueous foam > Alumi-static > Alumi-slow > Alumi-fast. The difference between the foams can be explained based on the cell shape shown in Figure 1: many cells in Alumi-fast and Alumi-slow are tadpole-like and have small tails, which causes their poor sphericity and larger anisotropy, the reason for which will be discussed in Section 4. Cells of Alumi-static are polyhedral because of the larger cell size combined with a lower foam density. Bubbles of the Aqueous foam are nearly spherical. One reason for this is that the bubbles are smaller and their stability is guaranteed by the surfactants in the aqueous solution; another is that the Aqueous foam was scanned in the liquid state and the decrease of the liquid fraction by drainage was limited.

## 2.2. Cells Stacking Status of the Foam Samples

### 2.2.1. Coordination Number

Coordination numbers of nonborder cells in the four samples were calculated, and their distribution frequency is shown in **Figure 4**. The peak coordination number of all samples is 12; especially the distribution frequency with a cell coordination number of 12 reaches 85% for the Aqueous foam. Alumi-fast has the most concentrate distribution with a peak of 12 among the three aluminum foams. The cell coordination number distribution of Alumi-slow is a little wider than that of Alumi-fast, and has another peak at 11. The distribution of Alumi-static is very broad, and the second peak position is located at 14. The coordination numbers of cells in each foam are distributed and smaller coordination numbers are generally due to locally thicker walls mainly caused by vacancies formed during bubble accumulation. Larger coordination numbers than 12 are usually accompanied by a sacrifice in cell sphericity or size uniformity because bubbles always tend to be densely packed for reduced free energy.
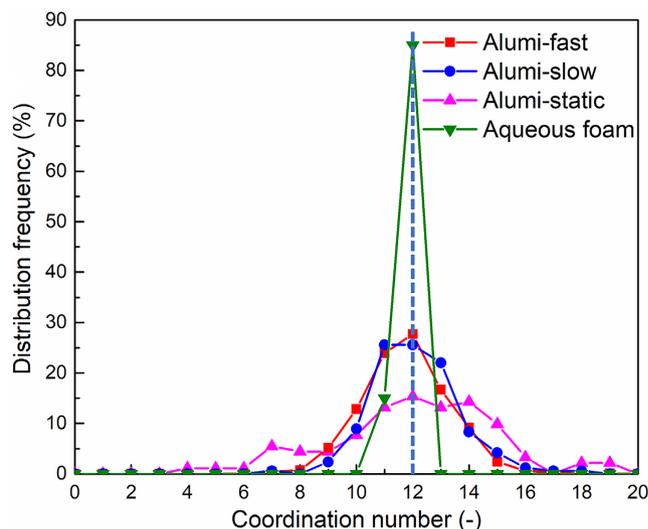
Therefore, Aqueous foam and Alumi-fast are more like ideal close-packed structures (FCC or HCP) in terms of coordination number, and cells in these two foams are expected to be in ordered stacking.

### 2.2.2. Radial Distribution Function

The coordination number reflects the cell distribution in a close range around one cell. For studying the cell distribution in spheres at a more general distance along a given cell of the foam, namely, the cell structure at a longer range, the radial distribution function $g(r)$ of the four foams was analyzed. As expressed in Equation (1), $g(r)$ refers to the number of cell centers per unit volume in a sphere shell of thickness $dr$, where the distance between the sphere shell and the given sphere center is $r$.[14,26] In Equation (1), $n(r_1)$ and $n(r_2)$ are the number of cell centers within spheres, where the distances to the given cell are $r_1$ and $r_2$, respectively.

$$n(r_2) - n(r_1) = \int_{r_1}^{r_2} g(r) 4\pi r^2 dr \qquad (1)$$

Based on the cell position coordinates of a foam, the cell located in the geometric center was found and taken as the starting cell, after which $g(r)$ can be obtained after ranking all cells according to their distance to that central cell. **Figure 5**a–d shows the normalized radial distribution functions of the four foam samples, wherein $d$ is the average equivalent diameter of all cells in the foam, and $g(r_0)$ is the first peak position of $g(r)$. Because there is a preference for FCC over HCP for sphere stackings,[27,36] the distribution of the ideal FCC structure is displayed in Figure 5 for comparison. The radial distribution function of an ideal FCC structure is discrete. The light-blue region in Figure 5a indicates that the first five peaks of $g(r)$ of Alumi-fast are consistent with that of FCC, so the cell distribution in an ≈2.5 cell diameter range appears densely stacked and ordered. For
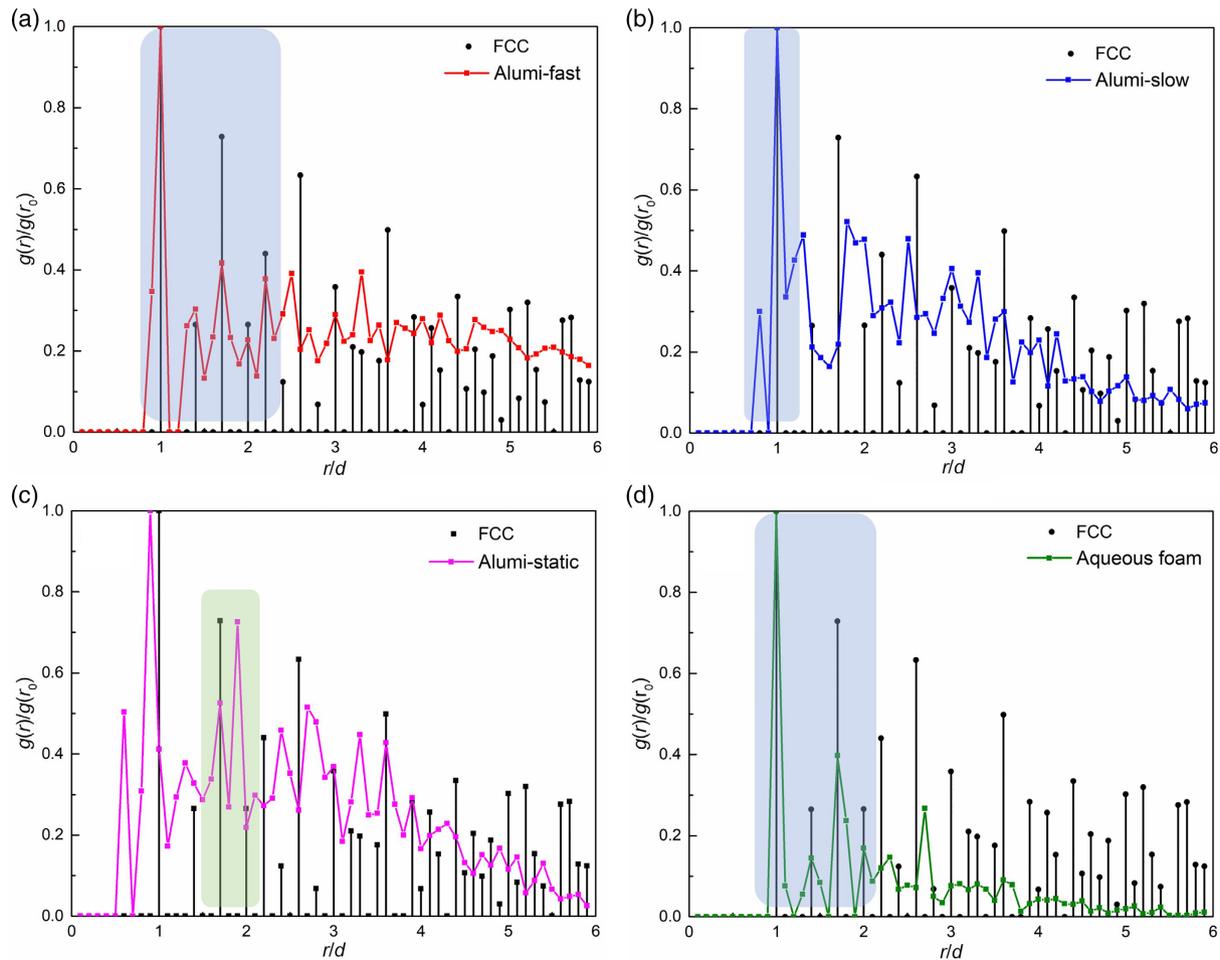
**Figure 5.** Normalized radial distribution function $g(r)$ of the four foam samples compared with an ideal FCC structure, a) Alumi-fast, b) Alumi-slow, c) Alumi-static, and d) Aqueous foam. The light-blue regions represent the peak locations consistent with the FCC structure in (a,b,d); the light-green region marks the two peaks located at $\sqrt{3}d$ and 1.9$d$ in (c).

Alumi-slow in Figure 5b, only the first peak of the normalized $g(r)$ is located at distance $d$, whereas the other peaks do not agree with that of the FCC structure. As shown in Figure 5c, the peak locations of the radial distribution function of Alumi-static are quite different from that of FCC, and the main peaks appear at $\sqrt{3}d$ and 1.9$d$ ($\approx 2d$) when the distance is between $d$ and $2d$ as marked by the light-green region. According to the description in the literature,[14,37] the cell stacking structure of Alumi-static meets the features of a disordered and random stacking of hard spheres. Combined with the previous analysis for the coordination number, Alumi-static should be a random stacking structure. The radial distribution function of the Aqueous foam in Figure 5d shows that the locations of its first four peaks are the same as those of the FCC structure and the low subsequent peaks limited by the fewer cells should be ignored.

Except for the radial distribution function based on the central cell of each foam in Figure 5, $g(r)$ with other cells as the starting cell in the four foams were also calculated. Although small differences in the diameter or shape of a given cell greatly affect the peak positions of the radial distribution function, more cells with

the first few peaks consistent with the FCC structure imply a more ordered structure of the foam. It has been found that the normalized radial distribution function of most cells in the Aqueous foam is similar to that in Figure 5d; namely, the first four peaks are consistent with that of the FCC structure. The radial distribution function of some cells can also reflect the short-ranged ordering state of Alumi-fast as in Figure 5a, even though the fraction of cells conforming to an ordered arrangement is less than that in the Aqueous foam. The peaks, except the first one of the radial distribution functions, of nearly all cells in Alumi-slow and Alumi-static, do not coincide with those of the FCC structure, so these two foams cannot be interpreted as ordered, even though the first peak of some cells is located at a distance of one diameter. Therefore, only the cell stacking structures of Alumi-fast and Aqueous foam are ordered in a certain range.

**Figure 6** shows the total number of cells $n(r)$ within a radial distance of $r$ around the central cell of the four foams and for the FCC structure. It corresponds to the integration of the radial distribution function, and can reflect the stacking efficiency of the
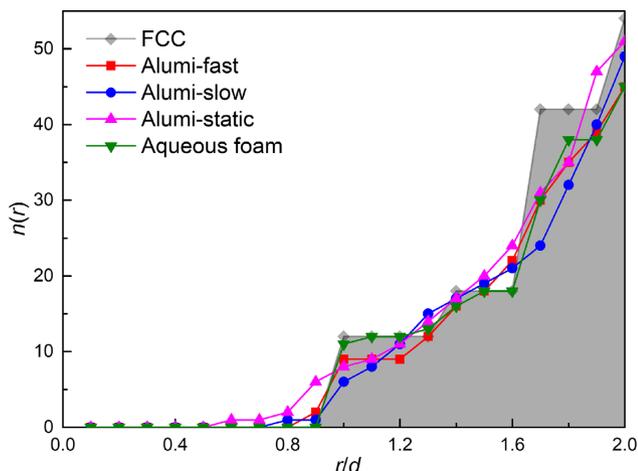
**Figure 6.** Total number of cell centers within a radial distance of $r$ around the central cell of the four foam samples and the FCC structure displayed as a function of $r/d$, where $d$ is the average cell equivalent diameter of the foams.

foams, namely, the local dense packing degree of cells.[14] As shown in Figure 6, the total number of cells contained in a sphere increases by leaps with increasing distance for the FCC structure.[14] There are two obvious steps when the radial distance $r$ is at $1d$–$1.3d$ and $1.4d$–$1.6d$ for the Aqueous foam and one step at $1d$–$1.3d$ for Alumi-fast, by which their short-range order is verified. The cell number increase over the radial distance of Alumi-static deviates most from the one of FCC because of its random stacking, followed by that of Alumi-slow.

### 2.2.3. Macroscopic Cross-Section of the Aluminum Foams

To further explore the manifestations of cell structure ordering in the aluminum foams, cross-sectional tomographic slices at the center of Alumi-fast and Alumi-slow are shown in **Figure 7**, where the stacking state of cells is illustrated more visibly in 2D sections. The image shows the whole solid sample, and can be divided into a lower foam with a conical structure and an upper foam with cylindrical structure, as separated by the blue lines in Figure 7. The conical foam shape is caused by the position of the gas injection orifice at the bottom center of the

crucible, and bubbles after detaching from the rotating orifice tend to impinge in the center under the influence of inertia force. For Alumi-fast in Figure 7a, porosities of the lower and upper foams are 65.4% and 70.5%, respectively; i.e., the bottom of the liquid foams in Figure 7 is wetter than the top because of the higher liquid fraction in this region caused by gravity. The upper foams are dryer, with closely packed fine cells after more sufficient drainage and self-adjustment of positions.

As shown in Figure 7a,b, there are several bubble chains aligned along the cone in the lower foam, and even more such chains can be observed in the upper foam. According to the marked red lines of some bubble chains, the chains are distributed over the entire section and mainly surround the foam center, which implies that the extension of the bubble chains is confined by the crucible wall. It was inferred that these bubble chains are caused by the interaction force between bubbles according to the packing analysis of emulsion drops and granular spheres.[38,39] The bubble chains for Alumi-fast are generally longer than those in Alumi-slow, and most of them have more than five bubbles in a row in the 2D section, which may signify that its cell stacking is more ordered. Similar bubble chains were also reported in other aluminum foams with small cells,[8] and the forming of bubble chains should reflect the ordering state to some extent. Therefore, the aluminum foam with uniform 1.2 mm sized cells was further proved to be an ordered foam structure within a short range.

## 3. Discussion

Cells in aluminum foam prepared by high-speed rotating gas injection (Alumi-fast) are ordered and densely arranged in a short range in terms of coordination number and radial distribution function similar to the Aqueous foam with almost mono-sized small bubbles. The degree of order is reduced for Alumi-slow. In addition, the cell stacking state of Alumi-static resembles more a random stacking. Monodisperse aqueous foam has been verified to be in an ordered dense packing after gas injection and before its self-organization.[22,23] Although liquid cells of aluminum foam should also be densely and ordered packed just after gas injection if the influence of the rotating needle is not considered, due to drainage previous to solidification it is not easy for the final aluminum foam structure to be ordered. The main difficulty for obtaining ordered aluminum foam is
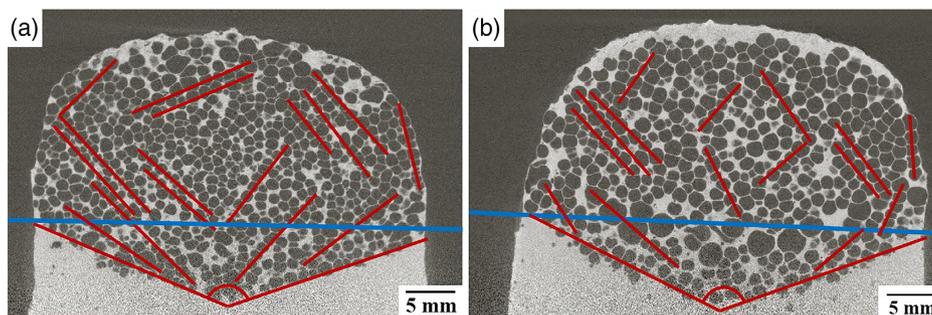


**Figure 7.** Cross-sectional tomography slices at the center of a) Alumi-fast and b) Alumi-slow. Red lines point at linear arrangements of cells.

controlling the cell size, size uniformity, and cell shape during preparation.

Influences of the cell features on ordered stacking are reflected by the three aluminum foams in this study. The random cell stacking state of Alumi-static is mainly caused by large and polyhedral cells. Membranes of larger bubbles are more easily deformed compared to smaller bubbles because of the smaller internal bubble pressure according to the Young–Laplace equation. Furthermore, the rise rate of smaller bubbles after detachment from the orifice is slower because a decrease in bubble diameter reduces the upward buoyancy more than it reduces the opposing viscous resistance. This allows them to choose a lower energy position during bubble accumulation.[25,36] The less ordered structure of Alumi-slow is primarily caused by its wide cell size distribution. The less uniform cell size causes the inconsistency with the peaks of the FCC structure in terms of the radial distribution function. In addition, many cells in Alumi-slow and Alumi-fast are tadpole-like, with small tails that are created when the bubble interior oxidizes at the gas/metal interface during bubble inflation and a neck is formed, which evolves into a tadpole-like shape after bubble detachment. This shape cannot relax back to the spherical shape during bubble rise due to the too rigid surface. The small average cell diameter and narrow cell size distribution of Alumi-fast contribute to its short-range order, although the small tails of cells lead to a lower sphericity and larger anisotropy and might prevent an even higher degree of order.

The order of aluminum foams could be improved considering the following aspects: 1) it has been found that the cell size of aluminum foam was significantly decreased when the size of the added ceramic particles was reduced from 10 to 3 μm and the addition was reduced to 7 vol%.[9] In addition, a higher rotation speed of the needle during gas injection should be more helpful for an earlier detachment of bubbles.[40] Therefore, the cell size of aluminum foam could be further reduced by evenly dispersing smaller ceramic particles in an aluminum melt and increasing the rotation speed of the gas injection needle. 2) Any disturbance of the melt potentially affects the uniformity of bubble size during gas injection. A more stable melt state could be obtained by using a gas injection needle with a smaller outer diameter, but this might weaken the needle strength and reduce its durability. 3) Bubbles will be elongated during detachment from an orifice rotating at high speed, and small tails will exist in the final cells if the initial elongation is not reversed during bubble rise, which is hindered by a too thick oxide film. The nonstraight path of rising bubbles and the slower rise velocity of small bubbles[41] in the high-speed gas injection system both cause the longer oxidation time of bubbles in the melt, resulting in a thick oxide film. It has been investigated that aluminum foams with complete and good cell structure can be obtained when the oxygen content of the injected gas is more than 1.6%, which is much less than the oxygen content in the synthetic air used.[42] Therefore, cell shapes could be improved by a controlled decrease of the oxygen content in the injected gas while maintaining a minimum necessary for bubble stability, and reducing the foaming temperature appropriately to delay the formation of oxide films. 4) As described in Section 3.2.3, the crucible wall will confine the extension of bubble ordering. The meniscus at the interface between air and the liquid will also affect the accumulation of bubbles.[25] Larger crucible dimensions could reduce these influences but more than one gas injection needle might have to be used simultaneously to ensure a high throughput in this case. The aforementioned methods should be adopted step by step to study their influence.

## 4. Conclusion

Three aluminum foam samples prepared by high-speed rotation (Alumi-fast), lower-speed rotation (Alumi-slow), and static (Alumi-static) gas injection and an aqueous foam in comparison were studied in this article. The following conclusions can be obtained by characterizing the resulting cell structures and cell stacking states quantitatively. 1) Because of the uniformly sized small cells (1.2 mm in diameter), Alumi-fast represents a foam structure with a pronounced short-range order reflected by i) concentrated distribution of cell coordination numbers with a peak of 12; ii) the first five peaks of the radial distribution function being consistent with that of the FCC structure; and iii) many aligned bubble chains with more than five bubbles being observed in the 2D cross-sectional images. 2) The cell stacking of Alumi-static is not ordered due to larger and polyhedral cells. The stacking state of Alumi-slow is limited by its poor cell size uniformity. Many cells of smaller sphericity and larger anisotropy in Alumi-fast prevent an even higher order.

Methods for improving the degree of order of aluminum foams include increasing the rotation speed of dynamic gas injection and reducing the ceramic particle size in the foamable melt to reduce the cell size; reducing the needle size to improve the melt stability during gas injection; and decreasing the oxygen volume fraction of injected gas.

## 5. Experimental Section

*Sample Preparation*: A metal matrix composite (MMC) containing AlSi9Mg0.6 alloy (in wt%) and 20 vol% stabilizing SiC particles of 10 μm nominal size was melted in a crucible. Separately melted commercial A359 alloy was then added to the liquid MMC to dilute the SiC particle content down to 11 vol%. Mechanical stirring was applied to evenly disperse the SiC particles.[8,9] A high-speed gas injection system rotating with up to 2000 rpm was applied to inject compressed air into the MMC melt held at 670 °C. The system contained a rotating cannula sealed at the bottom of the crucible. It had a 0.2 mm inner and a 0.5 mm outer diameter, and was bent to 45° so that its orifice described a circle of around 10 mm radius in the melt during rotation. The horizontal force on the gas bubble at the orifice of the cannula causes earlier detachment compared to a resting orifice; therefore, smaller bubbles are created. A detailed study of this technique including the influence of processing parameters was recently published elsewhere.[40]

Two aluminum foam samples prepared by this method were studied. The gas flow rates of the two samples were 30 and 70 mL min⁻¹, and the rotation speeds 2000 and 1400 rpm, so they are named *Alumi-fast* and *Alumi-slow*, respectively. High-speed rotation of a sufficiently thin cannula at the bottom of the crucible makes the detachment condition of each bubble as reproducible as possible and has little impact on the melt, thus improving the uniformity of bubbles while bubble size is reduced.

For comparing the influence of bubble size on the degree of ordering during accumulation, another foam prepared by static gas injection was studied, named *Alumi-static*. For its preparation, 10 vol% of 10 μm sized Al₂O₃ particles were added to the commercial A356 melt. Compressed air was injected into the foamable melt at 680 °C through a static needle. The

**ADVANCED
SCIENCE NEWS**
www.advancedsciencenews.com

**ADVANCED
ENGINEERING
MATERIALS**
www.aem-journal.com

smallest bubble size was obtained selecting a chamber pressure of 0.4 MPa and an orifice diameter of 0.25 mm. The preparation of this sample has been described in detail elsewhere.[10] Due to the large cell size of the aluminum foam prepared by static gas injection, a larger sample dimension was required to include a sufficient number of cells for studying the cell stacking structure. Therefore, another preparation system was utilized to obtain Alumi-static. The compositions of the matrix alloy and the amount of added ceramic particles are similar in the dynamic and static gas injection methods. Moreover, the matrix material and ceramic particles should have little effect on the final cell stacking structure as long as stable bubbles are generated during preparation; that is why the cell stacking of Alumi-static can be compared with those of Alumi-fast and Alumi-slow. Cell size uniformity of aluminum foams obtained by the static method was satisfying because of the same formation condition of each bubble. To avoid the formation of polyhedral cells as much as possible and to facilitate ordered accumulation, the cell size of Alumi-static was selected to be at the lower end of cell sizes that the static gas injection method can deliver.[10]

For comparison with aluminum foams, a stable, monodispersed *Aqueous foam* was prepared and characterized. An aqueous solution with 5 vol% detergent Fairy liquid was filled into a thin-walled tube made of polyimide, which had good X-ray transmission. Air mixed with perfluorohexane vapor was injected through a cannula of 0.2 mm inner diameter. The bubble size was controlled by adjusting the gas pressure. A similar preparation procedure has been described in the literature.[25] The surfactant and the insoluble perfluorohexane vapor improve the stability of bubbles by stabilizing the liquid films and avoiding gas diffusion through them, respectively.

*Characterization of Foam Structure*: The three aluminum foam samples were scanned by a laboratory X ray tomography equipment described in detail elsewhere.[43] The aqueous foam sample was measured at the beamline of the BESSY II synchrotron facility of Helmholtz-Zentrum Berlin. The 3D foam structure of the samples was obtained after reconstructing the projections collected by the X-ray detectors. Avizo software (FEI, USA) was used to extract the specific cell structure data. After the process steps of cutting, binarization, watershed segmentation, labeling, etc., the size and shape parameters of each cell could be attained, including volume, surface area, equivalent diameter, anisotropy, sphericity, barycenter, and orientation.[34] Based on these cell parameters, the 3D stacking state of each foam sample was analyzed.

The equivalent diameter, i.e., the diameter of a sphere with the same volume as a given cell, was used to evaluate the cell size in this article. There were some micropores or microbubbles in both aluminum and aqueous foams. They are mainly caused by the air present in the melt or by small bubbles escaping from the gas injection orifice due to disturbances. In addition, some dots with a few pixels in the matrix may also be recognized as micropores limited by resolution. Micropores were not considered in the cell stacking analysis, but are discussed in Section 3.1.

Sphericity and anisotropy were utilized to evaluate the cell shape from different aspects. Sphericity is the surface area ratio of a sphere and the cell with the same volume, and corresponds to 1 for an ideal sphere. Small sphericity of a cell means a large difference in surface area to an ideal sphere. The anisotropy of a perfect spherical cell is 0, and larger anisotropy means a larger difference of the smallest and largest eigenvalue of the covariance matrix of a cell, which indicates a larger deviation from spherical shape.

The coordination number was used to quantitatively describe the stacking condition of cells and to assess the ordering state of the foams. It refers to the number of neighbors of a cell or bubble in a foam. If the distance between the center of one cell and a target cell is not larger than the sum of their radii and a given wall thickness, this cell is counted as a neighbor of the target cell. Considering the wall between two cells and cell shape deviation from an ideal sphere, the thickness is defined as around 0.3 times the average cell diameter of the foam in this article. The coordination numbers of FCC and HCP are both 12—and both are ideal close-packed structures—whereas BCC has a coordination number of 8. Therefore, a foam with a cell coordination number of 12 is considered to be dense and ordered.

## Conflict of Interest

The authors declare no conflict of interest.

## Data Availability Statement

The data that support the findings of this study are available from the corresponding author upon reasonable request.

[1] J. Banhart, *Adv. Eng. Mater.* **2013**, *15*, 82.

[2] L. J. Gibson, M. F. Ashby, *Cellular Solids: Structure and Properties*, Cambridge University Press, Cambridge, NY **1997**.

[3] J. Banhart, *Prog. Mater. Sci.* **2001**, *46*, 559.

[4] F. García-Moreno, *Materials* **2016**, *9*, 85.

[5] T. Miyoshi, M. Itoh, S. Akiyama, A. Kitahara, *Adv. Eng. Mater.* **2000**, *2*, 179.

[6] F. Baumgärtner, I. Duarte, J. Banhart, *Adv. Eng. Mater.* **2000**, *2*, 168.

[7] Y. Zhou, Y. Li, J. Yuan, *Colloids Surf. A* **2015**, *482*, 468.

[8] F. García-Moreno, B. Siegel, K. Heim, A. J. Meagher, J. Banhart, *Colloids Surf. A* **2015**, *473*, 60.

[9] N. Wang, X. Chen, Y. Li, Z. Liu, Z. Zhao, Y. Cheng, Y. Liu, H. Zhang, *Colloids Surf. A* **2017**, *527*, 123.

[10] J. Yuan, Y. Li, N. Wang, Y. Cheng, X. Chen, *Metall. Mater. Trans. B* **2016**, *47*, 1649.

[11] X. Chen, N. Wang, J. Yuan, Y. Li, H. Zhang, Y. Liu, *J. Mater. Eng. Perform.* **2017**, *26*, 3307.

[12] I. Jin, L. D. Kenny, H. Sang, *USA Patent 4973358*, **1990**.

[13] D. Wang, Z. Shi, *Mater. Sci. Eng., A* **2003**, *361*, 45.

[14] T. Aste, M. Saadatfar, T. J. Senden, *Phys. Rev. E* **2005**, *71*, 061302.

[15] D. Weaire, T. Aste, *The Pursuit of Perfect Packing*, CRC Press, Boca Raton, FL **2008**.

[16] J. D. Bernal, J. L. Finney, *Discuss. Faraday Soc.* **1967**, *43*, 62.

[17] A. Mughal, H. K. Chan, D. Weaire, S. Hutzler, *Phys. Rev. E* **2012**, *85*, 051305.

[18] S. Pronk, D. Frenkel, *J. Chem. Phys.* **1999**, *110*, 4589.

[19] A. J. Meagher, F. García-Moreno, J. Banhart, A. Mughal, S. Hutzler, *Colloids Surf. A* **2015**, *473*, 55.

[20] W. Drenckhan, D. Langevin, *Curr. Opin. Colloid Interface Sci.* **2010**, *15*, 341.

[21] W. Drenckhan, S. Hutzler, *Adv. Colloid Interface Sci.* **2015**, *224*, 1.

[22] A. van der Net, D. Weaire, S. Hutzler, *Soft Matter* **2009**, *5*, 318.

[23] R. Höhler, Y. Yip Cheung Sang, E. Lorenceau, S. Cohen-Addad, *Langmuir* **2008**, *24*, 418.

[24] J. A. Glazier, S. P. Gross, J. Stavans, *Phys. Rev. A* **1987**, *36*, 306.

[25] F. García-Moreno, P. H. Kamm, T. Neu, K. Heim, A. Rack, J. Banhart, *Colloids Surf. A* **2017**, *534*, 78.

[26] A. J. Meagher, M. Mukherjee, D. Weaire, S. Hutzler, J. Banhart, F. Garcia-Moreno, *Soft Matter* **2011**, *7*, 9881.

[27] A. J. Meagher, D. Whyte, J. Banhart, S. Hutzler, D. Weaire, F. Garcia-Moreno, *Soft Matter* **2015**, *11*, 4710.

[28] D. Georgieva, A. Cagna, D. Langevin, *Soft Matter* **2009**, *5*, 2063.

[29] K. Heim, G. S. V. Kumar, F. Garcia-Moreno, I. Manke, J. Banhart, *Colloids Surf. A* **2013**, *438*, 85.

[30] N. Babcsan, S. Beke, P. Makk, *World Patent WO 2010/064059 A2*, **2010**.

[31] N. Babcsan, S. Beke, P. Makk, G. Szamel, C. Kadar, *Procedia Mater. Sci.* **2014**, *4*, 127.

[32] N. Babcsan, S. Beke, P. Makk, P. Soki, G. Számel, H. P. Degischer, R. Mokso, *13th Int. Conf. on Aluminum Alloys (ICAA13)*, Springer, Pittsburgh, USA **2012**, p. 1005.

[33] N. Wang, X. Chen, J. Yuan, G. Wang, Y. Li, H. Zhang, Y. Liu, *Metall. Mater. Trans. B* **2016**, *47*, 3362.

[34] N. Wang, X. Chen, E. Maire, P. H. Kamm, Y. Cheng, Y. Li, F. García-Moreno, *Adv. Eng. Mater.* **2020**, *22*, 2000264.

[35] N. Wang, E. Maire, Y. Cheng, Y. Amani, Y. Li, J. Adrien, X. Chen, *Mater. Charact.* **2018**, *138*, 296.

[36] S. Heitkam, W. Drenckhan, J. Frohlich, *Phys. Rev. Lett.* **2012**, *108*, 148302.

[37] J. L. Finney, *Proc. R. Soc. London A* **1970**, *319*, 479.

[38] A. Giustiniani, S. Weis, C. Poulard, P. H. Kamm, F. García-Moreno, M. Schroter, W. Drenckhan, *Soft Matter* **2018**, *14*, 7310.

[39] J. L. Anthony, C. Marone, *J. Geophys. Res.* **2005**, *110*, B08409.

[40] M. A. Noack, F. Bülk, N. Wang, J. Banhart, F. García-Moreno, *Mater. Sci. Eng., B* **2021**, *273*, 115427.

[41] R. H. Jean, L. S. Fan, *Chem. Eng. Sci.* **1990**, *45*, 1057.

[42] Y. Zhou, Y. Li, *Trans. Nonferrous Met. Soc. China* **2015**, *25*, 2429.

[43] F. García-Moreno, M. Fromme, J. Banhart, *Adv. Eng. Mater.* **2004**, *6*, 416.